Title

Structure and Solution Dynamics of Lithium Methyl Carbonate as a Protective Layer For Lithium Metal

Journal

ACS Applied Energy Materials, 1(5)

ISSN

2574-0962

Authors

Liu, Haodong
Wang, Xuefeng
Zhou, Hongyao
et al.

Publication Date

2018-05-29

DOI

10.1021/acsaem.8b00348

Peer reviewed

ACS APPLIED ENERGY MATERIALS
Cite This: ACS Appl. Energy Mater. XXXX, XXX, XXX−XXX
Letter
www.acsaem.org

Structure and Solution Dynamics of Lithium Methyl Carbonate as a Protective Layer For Lithium Metal

Haodong Liu,[†] Xuefeng Wang,[†] Hongyao Zhou,[†] Hee-Dae Lim,[†] Xing Xing,[†] Qizhang Yan,[†] Ying Shirley Meng,[†,‡] and Ping Liu*[,†,‡]

[†]Department of NanoEngineering, University of California San Diego, La Jolla, California 92093, United States
[‡]Sustainable Power and Energy Center, University of California San Diego, La Jolla, California 92093, United States

Supporting Information

ABSTRACT: Lithium methyl carbonate (LMC) is synthesized in a single step and investigated as a coating material for Li protection. The LMC layer can be formed *in situ* during Li plating on Cu foil. The chemical and crystal structure of the ∼1 μm thick coating is confirmed, which remains intact during lithium cycling. SEM also confirms the dissolution of the LMC layer after being transferred into the commercial $LiPF_6$-carbonate electrolyte. Presaturating the electrolyte with LMC powder prevents the dissolution of the LMC coating layer, which improves the Li plating/stripping Coulombic efficiency from 90.5% (bare Cu in commercial electrolyte) to 96.1% at 0.5 mA cm^{-2} and 1 mAh cm^{-2}.

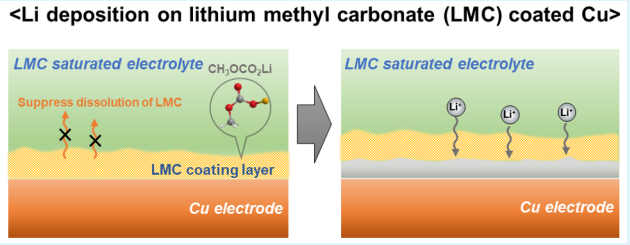

KEYWORDS: *single-component coating, Li metal anode, dendrite free, lithium methyl carbonate, LiI, solubility equilibrium*

1. INTRODUCTION

Although Li metal possesses the lowest electrochemical potential (−3.040 V vs SHE) and an extraordinarily high theoretical specific capacity (3860 mAh g^{-1}), the dendritic growth during repeated Li plating/stripping and low Coulombic efficiency prevents its use in practical applications.[1,2] Li metal is highly reactive, reacting with both Li containing salts and organic solvents in the electrolyte.[2] As a consequence, there are a variety of side reaction products that accumulate on the Li metal surface upon electrochemical cycling. Li dendrite growth is promoted due to the spatial nonuniform distribution of these side reaction products such as LiF, Li_2CO_3, ROLi, and RCO_2Li, that affect the uniformity of the Li ion flux.[3] The continuous evolution of the dendritic morphology increases the surface area of Li and creates isolated Li, which results in low Coulombic efficiency.[1,4−6] Strategies being proposed either reduce the reactivity of the electrolyte, or prevent the direct exposure of Li to the electrolyte in order to protect the Li. The success of concentrated electrolyte is attributed to the formation of a LiF-rich SEI layer and minimization of free solvent molecules.[7] *Ex situ* coating the Li surface with an artificial layer by a solution process, gas phase reaction, and atomic layer deposition are methods that effectively enhanced the reversibility of Li metal.[8−11] However, most of these coating materials react with Li metal. The reactions form an SEI layer between the coating and Li metal, resulting in complex compositions and microstructures which often correlate with nonuniform Li metal deposition.

Lithium alkyl carbonates are common organic SEI components in carbonate based electrolytes. Recognizing their potential chemical inertness with Li, we first introduced these as a protection layer for Li metal anode.[12] We hypothesized that the chemical uniformity will help maintain a more uniform current distribution and promote smooth Li deposition. We developed a facile one-step method that enables *in situ* formation of a lithium methyl carbonate (LMC) coating as a Li protection layer in LiI-EC/DMC electrolyte. This coating layer effectively suppresses the Li dendrite growth during repeated plating and stripping of Li. In this work, we aim to address three outstanding questions regarding the LMC coating layer: (1) What are the morphology and chemistry of the coating, and is there really no other SEI layer? (2) What is the Li metal cycling Coulombic efficiency (CE) in commercial $LiPF_6$-carbonate electrolyte with the help of this LMC coating? (3) How do the LMC solution dynamics affect the Li cycling Coulombic efficiency since LMC is likely to have some solubility in organic electrolytes? Our cryo-TEM results show that the LMC is indeed the only component on the deposited Li surface. We also confirmed the solubility of LMC. Besides the surface LMC layer, the LMC is also added into the commercial $LiPF_6$-carbonate electrolyte to manage the solution dynamics. This coating-solution saturation strategy suppresses the Li dendrite growth and improves the Li CE at the same time.

Received: March 5, 2018
Accepted: May 4, 2018
Published: May 4, 2018

DOI: 10.1021/acsaem.8b00348
ACS Appl. Energy Mater. XXXX, XXX, XXX−XXX

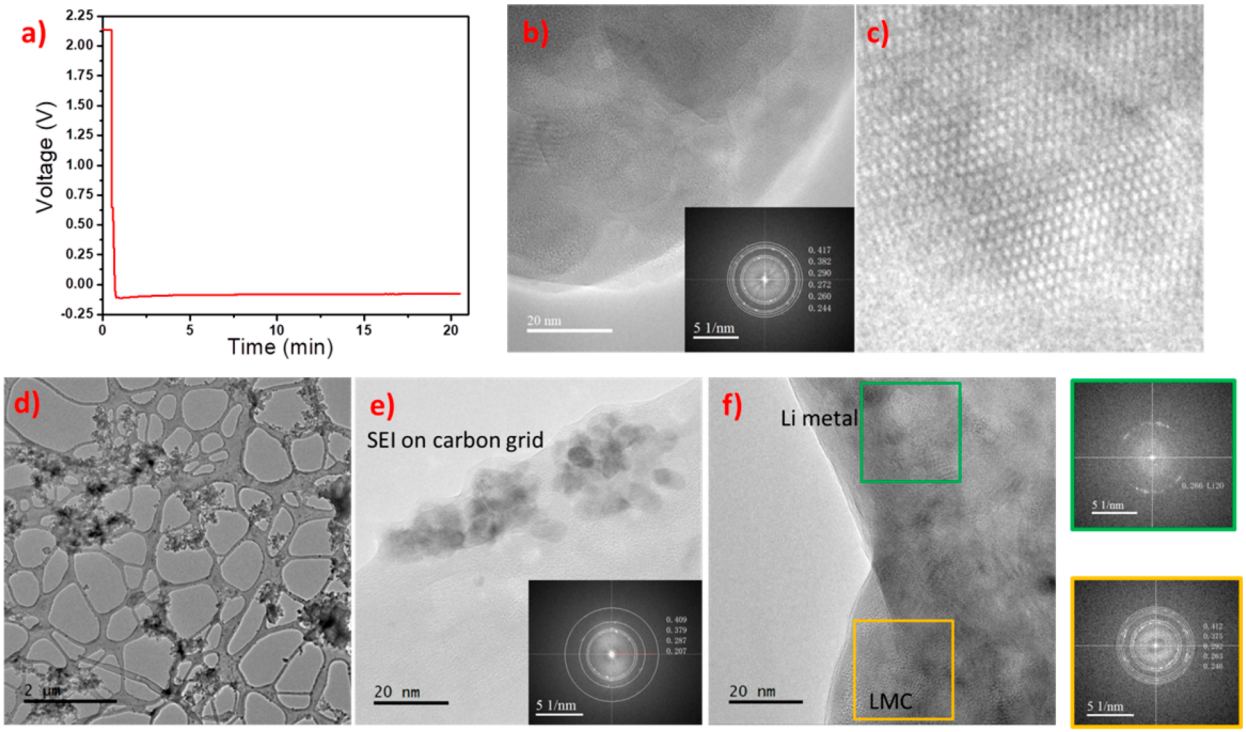

Figure 1. (a) Voltage profiles of Li plating on lacey carbon grid in 0.2 M LiI-EC/DMC electrolyte, 0.5 mA cm^{-2} for 20 min. (b, c) Cryo-TEM images of the LMC powders from the reaction between LiI and DMC. (d–f) Cryo-TEM images of the Li from the 0.2 M LiI-EC/DMC electrolyte after 20 min deposition at 0.5 mA cm^{-2}.

2. RESULTS AND DISCUSSION

Iodide ion is a well-known nucleophilic reagent that attacks the methyl group of DMC via a nucleophilic substitution reaction. Figure S1a shows the one-step reaction equation in which the LiI reacts with DMC to generate CH_3OCO_2Li (LMC) precipitates. According to our previous study on LiI-carbonate electrolyte, both DMC and mixed EC/DMC solvent could react with LiI and produce pure LMC precipitates.[12] The LMC powders prepared though DMC and EC/DMC were characterized by XRD. Figure S1b shows that the LMC from DMC solvent possesses sharp peaks, indicating it has a highly crystalline structure. On the other hand, the XRD peaks of LMC from the EC/DMC solvent were broad, which suggested a low degree of crystallinity. FTIR analysis was also carried out on both materials to further identify their chemical bonding information. Figure S1c is the comparison of the FTIR spectrum between the two LMC powders. Both LMC powders showed almost identical chemical bonds. The details on peak identification are described in the Supporting Information. All the XRD and FTIR peaks of both LMC powders are consistent with the LMC from Xu's work and confirm that the pure LMC powders are successfully synthesized by the facile one-step reaction.[12−15]

In our previous Li−Li symmetric cell study, a thick LMC coating layer was observed on the Li metal surface during repeated Li plating/stripping inside a LiI-EC/DMC electrolyte.[12] In order to investigate the microstructure and chemical composition of this coating layer, and in particular to examine whether there are other compounds at the interface, cryo-TEM was conducted on both LMC powder and electrodeposited Li covered with the LMC layer. The Li metal deposition sample for TEM was prepared in a Li−Cu type coin cell,[16] in which a lacey carbon grid was placed on top of the Cu foil and used as a substrate in a 0.2 M LiI-EC/DMC electrolyte. As shown in Figure 1a, the Li metal was plated at 0.5 mA cm^{-2} for 20 min. As a reference, Figure 1b,c shows the TEM images of LMC powders, which indicate the synthesized LMC has good crystallinity. Figure 1d–f show the TEM images of deposited Li on a lacey carbon grid. The low magnification image shows an agglomerated Li morphology instead of dendritic Li. The fast Fourier transform (FFT) pattern of Figure 1e shows clear diffraction rings, which are identical to the FFT pattern of LMC powder. All the diffraction rings are indexed to the LMC structure, except for the one at 0.417 nm which belongs to the Li_2CO_3. The slight amount of Li_2CO_3 that is not detected by XRD may come from the LMC reacting with the H_2O residue in the electrolyte. Figure 1f shows the interface and the surface parts of a deposited Li layer that was investigated. The FFT image of these regions suggests the pure LMC was formed on the surface of Li. The cryo-TEM on the deposited Li proved that the LMC was the only chemical species *in situ* generated on the Li surface as a coating layer during Li plating. In addition, benefiting from this chemical homogeneous coating layer, the plated Li showed a dendrite free morphology.

The LiI-EC/DMC electrolyte enables dendrite free Li morphology due to the formation of an LMC coating on the Li surface, which offers a highly uniform Li-ion flux through the layer.[12] This *in situ* generated layer that covered the Li surface was also supposed to suppress the side reaction between Li and electrolyte. As a result, this LMC coating layer was expected to improve the Li cycling Coulombic efficiency. The Li metal anode Coulombic efficiencies (CEs) in different electrolytes were evaluated by assembling Li−Cu coin cells. The testing protocol from Adam's work was followed to measure the Li metal CE, which is described in Supporting Information with details.[17] Figure S2 presents the voltage profiles of Li plating/

DOI: 10.1021/acsaem.8b00348
ACS Appl. Energy Mater. XXXX, XXX, XXX−XXX

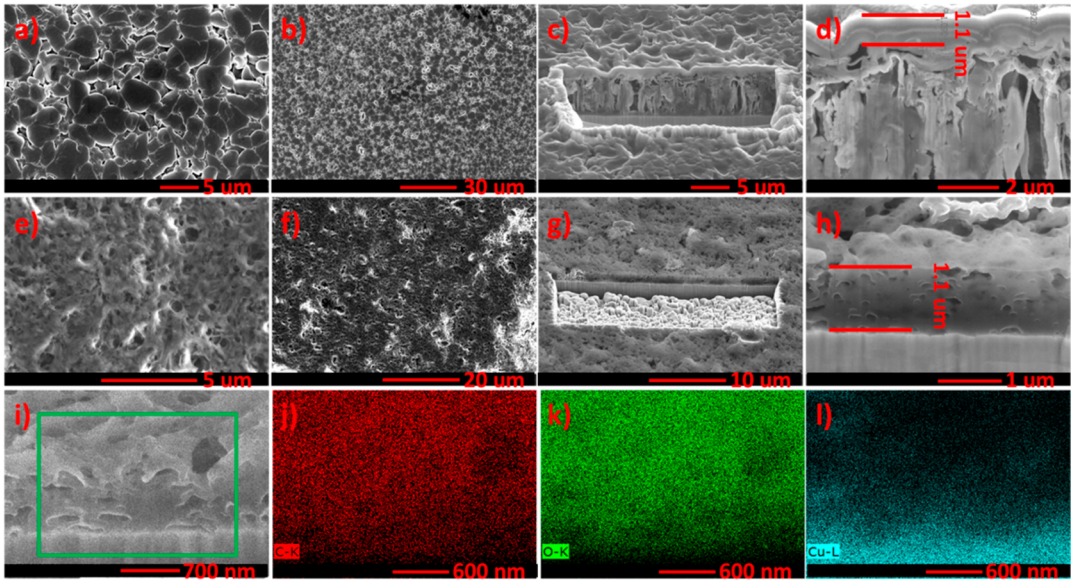

Figure 2. SEM images of LMC coated Cu foil. (a, b) Top view and (c, d) cross section view of Cu after 2 h of Li deposition at 0.5 mA cm^{-2} in 0.2 M LiI-EC/DMC electrolyte. (e, f) Top view and (g–i) cross section view of Cu after 2 h Li deposition at 0.5 mA cm^{-2}, then stripped to 1 V in 0.2 M LiI-EC/DMC electrolyte. (j–l) EDS elemental mapping of carbon, oxygen, and copper in part i, respectively.

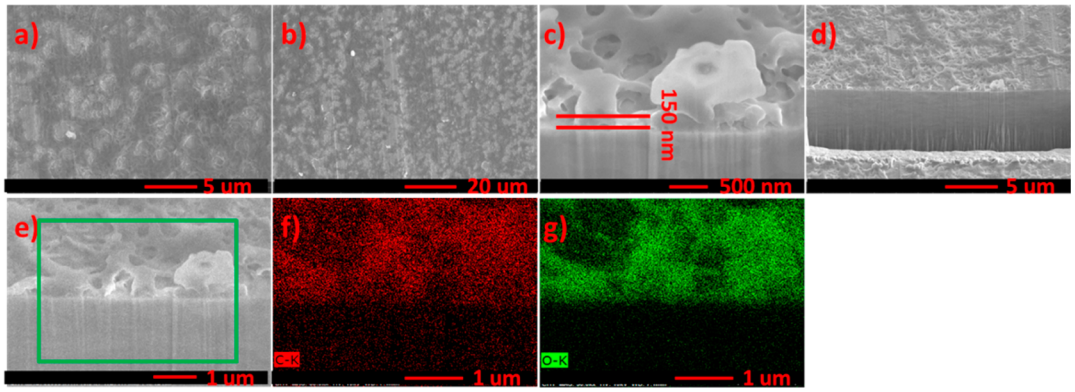

Figure 3. SEM images of LMC coated Cu foil after soaking into the EC/DMC for 24 h. (a, b) Top view and (c–e) cross section view of Cu. (f, g) EDS elemental mapping of carbon and oxygen in part e, respectively.

stripping in 1 M $LiPF_6$-EC/DMC (LP30), 0.1 M LiI-EC/DMC, and 0.2 M LiI-EC/DMC electrolyte, where their CEs are 90.9%, 91.8%, and 96.6%, respectively. The commercial LP30 electrolyte shows the lowest CE, due to the growth of a large amount of dendrites that promote the reaction between Li and electrolyte.[16] The higher LiI concentration electrolyte delivers a much improved CE of 96.6%. The CE enhancement in LiI based electrolyte indicates that the LMC coating effectively protects the Li metal.

Unfortunately, the operation voltage of those LiI based electrolytes is limited by the redox potential of I_3^-/I^-, which is far below the working potential (>4 V vs Li^+/Li) of common high energy density oxide cathode materials. Instead of directly using the LiI-EC/DMC electrolyte, our coating approach is applied to generate a protection layer of LMC on the Li metal surface. In order to coat the Cu substrate, a Li–Cu coin cell was assembled with 0.2 M LiI-EC/DMC electrolyte, and Li was plated on the Cu substrate at 0.5 mA cm^{-2} for 2 h, followed by complete stripping. The LMC coated Cu sample was obtained by disassembling the cell followed by quickly rinsing in DMC to remove the residual LiI. The morphology of plated Li on the Cu is shown in Figure 2a–d. The top view SEM images showed dendrite free morphology, while the cross section clearly illustrated three distinguishable regions: the Cu substrate, plated Li layer, and *in situ* formed LMC coating layer. Li grew vertically on the Cu substrate without any evidence of dendritic morphology; however, there were certain amounts of void spaces among the deposited Li. On top of the Li was the LMC coating layer, which capped the Li. The thickness of this LMC coating layer is ~1.1 μm. Figure 2e–h shows the SEM images of Cu substrate after fully stripping the Li. The top view images reveal that the coating layer is still on the Cu, but shows some porosity. The porous structure is also observed in the cross sectional images. The thickness of the LMC coating is maintained at ~1.1 μm. The EDS elemental mapping of its cross section shows strong signals of carbon and oxygen, which also confirms the existence of the LMC coating layer.

Tasaki investigated the solubility of Li salts in organic solvent through atomistic computer simulations.[18] The theoretical studies indicate all the Li salts found in the anode SEI, for example, lithium methoxide ($LiOCH_3$), lithium methyl carbonate ($LiOCO_2CH_3$), lithium ethyl carbonate ($LiOCO_2C_2H_5$), and dilithium ethylene glycol dicarbonate ($[CH_2OCO_2Li]_2$), have certain solubility in different organic

DOI: 10.1021/acsaem.8b00348
ACS Appl. Energy Mater. XXXX, XXX, XXX–XXX

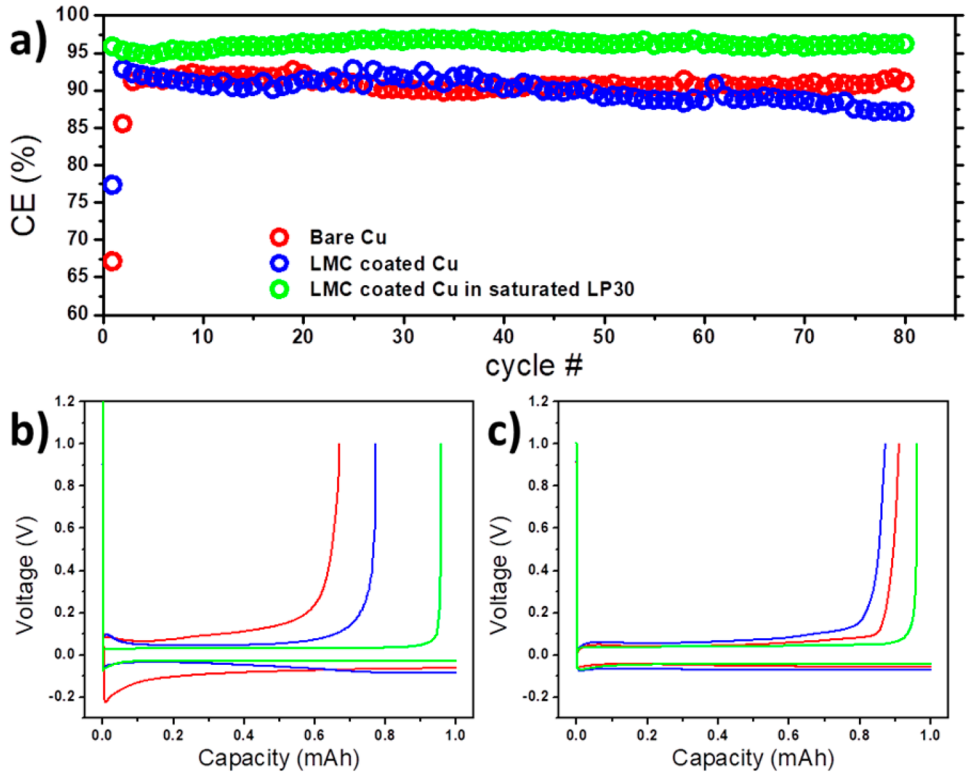

Figure 4. (a) Coulombic efficiency comparison of LillCu cell cycled in LP30 electrolyte at 0.5 mA cm^{-2} for 1 mAh cm^{-2}. (b) The first cycle voltage profiles. (c) The 80th cycle voltage profiles. (Red, bare Cu; blue, LMC coated Cu; green, LMC coated Cu in LMC saturated LP30.)

Scheme 1. (a) Li Plating on Cu in a Carbonate Electrolyte Results in Dendrite Growth, (b) The LMC Coating on Cu Partially Dissolves in the Carbonate Electrolyte and Reduces but Does Not Eliminate Dendrite Formation, and (c) in LMC Saturated Carbonate Electrolyte, Dissolution of the LMC Coating on Cu Is Suppressed Which Minimizes Dendrite Formation

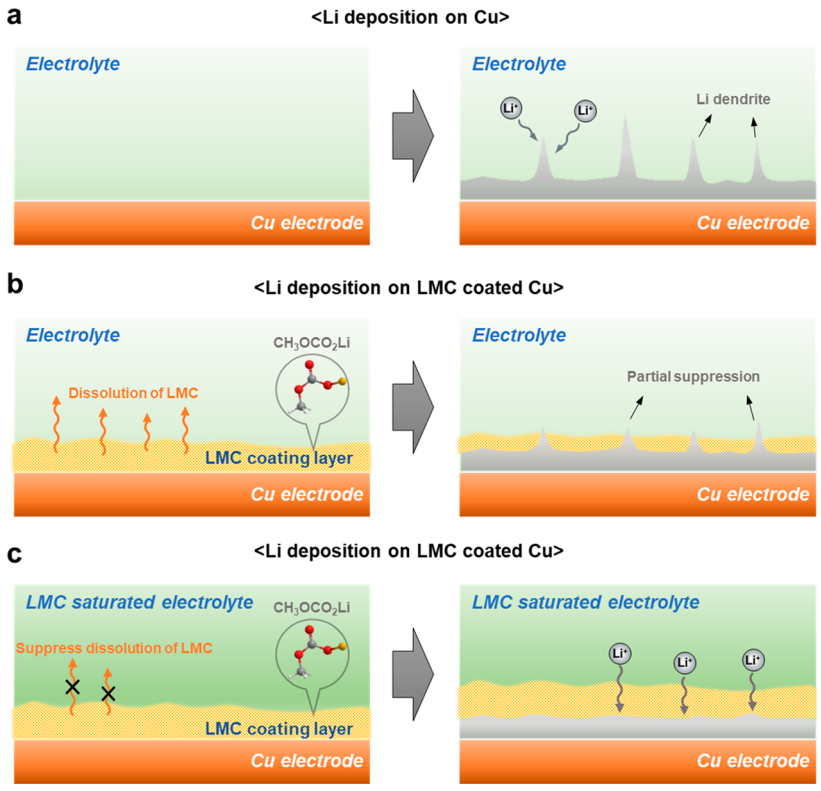

solvents. The solution dynamics of these key SEI components directly affects the stability, composition, and microstructure of the SEI film on the anode. The LMC is one of the common organic components in the solid electrolyte interphase on the

DOI: 10.1021/acsaem.8b00348
ACS Appl. Energy Mater. XXXX, XXX, XXX−XXX

surface of negative electrodes. In order to check the sustainability of the LMC coating layer in organic solvents, the LMC coated Cu was soaked in EC/DMC for 24 h. Figure 3 shows the morphology of the soaked LMC coating layer where the porous features still exist, while the thickness of the coating layer significantly decreases to 150 nm. More than 80% of the LMC coated on Cu has dissolved into the EC/DMC solvent in a short period of time. This is a direct observation of the SEI component dissolving into the organic solvent. The severe dissolution of LMC has to be prevented before it is applied as a protection layer for Li metal. The LMC powders from the reaction between LiI and DMC are used as an electrolyte additive for controlling the solubility equilibrium of LMC inside a battery.

The effects of LMC coating on the Li metal CE are investigated by testing the Li−Cu cells. The bare Cu cycled in LP30 electrolyte was chosen as a baseline. The LMC coated Cu was cycled in both LP30 and LMC presaturated LP30. The Li was plated on the Cu substrate at 0.5 mA cm^{-2} for 2 h, and then stripped at 0.5 mA cm^{-2} until the cell potential reached 1 V. This plating and stripping process was repeated for 80 times. Figure 4 shows the comparison of Li CEs and voltage profiles for the three cases. The LMC coated Cu delivered higher first cycle CE than the bare Cu. The CEs for bare Cu, LMC coated Cu, and coated Cu in LMC presaturated electrolyte are 67.1%, 77.3%, and 95.9%, respectively. In addition, the LMC coated Cu cycled in LMC presaturated LP30 exhibited higher CE than the bare Cu cycled in LP30 in repeated cycling. The average CE for 80 cycles of bare Cu in LP30 was 90.5%, while the LMC coated Cu in LMC presaturated LP30 delivered a much higher CE of 96.1%. In comparison, due to the gradual dissolution of the LMC coating layer, the LMC coated Cu cycled in LP30 only showed an advantage over the bare Cu for a few cycles. The morphology of deposited Li after 15 cycles was examined by SEM. Figure S3a−c shows the LMC coated Cu in LMC presaturated electrolyte, and Figure S3d,e shows the LMC coated Cu in LP30. The Li morphology in LMC presaturated electrolyte is dominated by agglomerated particles with minimal amounts of dendrite, while only dendritic Li was found on the LMC coated Cu from LP30. The cross sectional images revealed that, without the LMC additive in the electrolyte, the deposited Li possesses higher porosity.

Scheme 1 illustrates the working mechanisms for the LMC coating layer and LMC electrolyte additive. In LP30 electrolyte, the Li reacts with both solvent and $LiPF_6$, generating chemically complex SEI. The SEI is a mixture of ROLi, $ROCO_2Li$, LiF, Li_2O, Li_2CO_3, etc. These different compounds will likely lead to nonuniform electric fields at the Li and SEI interface, resulting in Li dendrite growth over the course of long-term cycling. In addition, the SEI continues breaking and forming during repeated Li plating and stripping caused by the large volume change of the Li. As a result, the electrolyte is gradually consumed in each cycle, and the Coulombic inefficiency increased. Scheme 1b shows the LMC coating layer on Cu dissolves into the organic solvent, and the dendritic Li grows on this coated Cu after a short period. In Scheme 1c, adding the LMC powder into the LP30 suppressed the LMC coating layer dissolution, although it is likely that the LMC coating layer and the LMC-saturated electrolyte are in a dynamic dissolution and deposition equilibrium process. This stable coating layer is chemically well-defined, which likely provides a uniform Li plating or stripping process and protects the Li from direct contact with the electrolyte. This LMC coating method combined with saturation of LMC in commercial electrolyte enables the dendrite free Li cycling with enhanced CE. Further investigation on employing the coated Li electrode in a full cell with a high voltage cathode will be included in our future work.

3. CONCLUSION

In summary, we have developed a one-step reaction between LiI and DMC to produce LMC. This reaction is used to coat Cu with a protection layer of pure LMC, which is supported by the cryo-TEM observations. This LMC coating layer is beneficial for both dendrite free Li cycling and high CE. Moreover, FIB-SEM shows this LMC coating layer loses thickness once it is soaked into EC/DMC, which reveals that it dynamically dissolves into the carbonate electrolyte. As a result, this LMC coating cannot enable long-term Li metal cycling. In order to enhance the sustainability of the LMC coating layer in commercial electrolytes, the LMC powder is used to presaturate the organic solvent. As a consequence of the two strategies, the Li CE in a commercial carbonate electrolyte is significantly improved from 90.5% to 96.1%. These findings provide new insights on designing effective protection layers and managing sustainable SEI formation for stable Li cycling.

4. EXPERIMENTAL METHODS

Refer to the Supporting Information for experimental details.

■ ASSOCIATED CONTENT

Supporting Information

The Supporting Information is available free of charge on the ACS Publications website at DOI: 10.1021/acsaem.8b00348.

Experimental methods; XRD and ATIR spectra of precipitates from LiI-DMC and LiI-EC/DMC; comparison of Li|Cu cell voltage profiles cycled in LP30, 0.1 M LiI-EC/DMC, and 0.2 M LiI-EC/DMC electrolytes; and SEM images of plated Li on LMC coated Cu foil after 15 repeating plating and stripping (PDF)

■ AUTHOR INFORMATION

Corresponding Author

*E-mail: piliu@eng.ucsd.edu (P.L.).

ORCID

Xuefeng Wang: 0000-0001-9666-8942

Ying Shirley Meng: 0000-0001-8936-8845

Ping Liu: 0000-0002-1488-1668

Author Contributions

P.L. and H.D.L. conceived the idea. H.D.L. performed electrochemical experiments. X.W. performed TEM experiments. All authors contributed to the writing of the manuscript and have given approval to the final version of the manuscript.

Notes

The authors declare no competing financial interest.

■ ACKNOWLEDGMENTS

This work was supported by the Office of Vehicle Technologies of the U.S. Department of Energy through the Advanced Battery Materials Research (BMR) Program (Battery500 Consortium) under Contract DE-EE0007764. Part of the work used the UCSD-MTI Battery Fabrication Facility and the UCSD-Arbin Battery Testing Facility. We acknowledge the UC Irvine Materials Research Institute (IMRI) for the use of the Cryo-Electron Microscopy Facility, which is funded in part by

DOI: 10.1021/acsaem.8b00348
ACS Appl. Energy Mater. XXXX, XXX, XXX−XXX

the National Science Foundation Major Research Instrumentation Program under Grant CHE-1338173.

REFERENCES

(1) Zhang, X. Q.; Cheng, X. B.; Zhang, Q. Advances in Interfaces Between Li Metal Anode and Electrolyte. *Adv. Mater. Interfaces* **2018**, *5*, 1701097.
(2) Cheng, X. B.; Zhang, R.; Zhao, C. Z.; Zhang, Q. Toward Safe Lithium Metal Anode in Rechargeable Batteries: A Review. *Chem. Rev.* **2017**, *117*, 10403−10473.
(3) Xu, W.; Wang, J. L.; Ding, F.; Chen, X. L.; Nasybulin, E.; Zhang, Y. H.; Zhang, J. G. Lithium Metal Anodes for Rechargeable Batteries. *Energy Environ. Sci.* **2014**, *7*, 513−537.
(4) Lin, D.; Liu, Y.; Cui, Y. Reviving the Lithium Metal Anode for High-Energy Batteries. *Nat. Nanotechnol.* **2017**, *12*, 194−206.
(5) Xu, K. Electrolytes and Interphases in Li-Ion Batteries and Beyond. *Chem. Rev.* **2014**, *114*, 11503−11618.
(6) Tikekar, M. D.; Choudhury, S.; Tu, Z.; Archer, L. A. Design Principles for Electrolytes and Interfaces for Stable Lithium-Metal Batteries. *Nature Energy* **2016**, *1*, 16114.
(7) Qian, J. F.; Xu, W.; Bhattacharya, P.; Engelhard, M.; Henderson, W. A.; Zhang, Y. H.; Zhang, J. G. Dendrite-Free Li Deposition Using Trace-Amounts of Water as an Electrolyte Additive. *Nano Energy* **2015**, *15*, 135−144.
(8) Li, N. W.; Yin, Y. X.; Yang, C. P.; Guo, Y. G. An Artificial Solid Electrolyte Interphase Layer for Stable Lithium Metal Anodes. *Adv. Mater.* **2016**, *28*, 1853−1858.
(9) Lin, D. C.; Liu, Y. Y.; Chen, W.; Zhou, G. M.; Liu, K.; Dunn, B.; Cui, Y. Conformal Lithium Fluoride Protection Layer on Three-Dimensional Lithium by Nonhazardous Gaseous Reagent Freon. *Nano Lett.* **2017**, *17*, 3731−3737.
(10) Kozen, A. C.; Lin, C. F.; Pearse, A. J.; Schroeder, M. A.; Han, X. G.; Hu, L. B.; Lee, S. B.; Rubloff, G. W.; Noked, M. Next-Generation Lithium Metal Anode Engineering via Atomic Layer Deposition. *ACS Nano* **2015**, *9*, 5884−5892.
(11) Lim, H. D.; Lim, H. K.; Xing, X.; Lee, B. S.; Liu, H.; Coaty, C.; Kim, H.; Liu, P. Solid Electrolyte Layers by Solution Deposition. *Adv. Mater. Interfaces* **2018**, *5*, 1701328.
(12) Liu, H. D.; Zhou, H. Y.; Lee, B. S.; Xing, X.; Gonzalez, M.; Liu, P. Suppressing Lithium Dendrite Growth with a Single-Component Coating. *ACS Appl. Mater. Interfaces* **2017**, *9*, 30635−30642.
(13) Xu, K.; Zhuang, G. R. V.; Allen, J. L.; Lee, U.; Zhang, S. S.; Ross, P. N.; Jow, T. R. Syntheses and Characterization of Lithium Alkyl Mono- and Dicarbonates as Components of Surface Films in Li-Ion Batteries. *J. Phys. Chem. B* **2006**, *110*, 7708−7719.
(14) Gireaud, L.; Grugeon, S.; Laruelle, S.; Pilard, S.; Tarascon, J. M. Identification of Li Battery Electrolyte Degradation Products through Direct Synthesis and Characterization of Alkyl Carbonate Salts. *J. Electrochem. Soc.* **2005**, *152*, A850−A857.
(15) Aurbach, D.; Daroux, M. L.; Faguy, P. W.; Yeager, E. Identification of Surface-Films Formed on Lithium in Propylene Carbonate Solutions. *J. Electrochem. Soc.* **1987**, *134*, 1611−1620.
(16) Wang, X. F.; Zhang, M. H.; Alvarado, J.; Wang, S.; Sina, M.; Lu, B. Y.; Bouwer, J.; Xu, W.; Xiao, J.; Zhang, J. G.; Liu, J.; Meng, Y. S. New Insights on the Structure of Electrochemically Deposited Lithium Metal and Its Solid Electrolyte Interphases via Cryogenic TEM. *Nano Lett.* **2017**, *17*, 7606−7612.
(17) Adams, B. D.; Zheng, J.; Ren, X.; Xu, W.; Zhang, J.-G. Accurate Determination of Coulombic Efficiency for Lithium Metal Anodes and Lithium Metal Batteries. *Adv. Energy Mater.* **2018**, *8*, 1702097.
(18) Tasaki, K.; Harris, S. J. Computational Study on the Solubility of Lithium Salts Formed on Lithium Ion Battery Negative Electrode in Organic Solvents. *J. Phys. Chem. C* **2010**, *114*, 8076−8083.

DOI: 10.1021/acsaem.8b00348
ACS Appl. Energy Mater. XXXX, XXX, XXX−XXX